This article has been accepted for publication in a future issue of this journal, but has not been fully edited. Content may change prior to final publication. Citation information: DOI 10.1109/LWC.2018.2810087, IEEE Wireless Communications Letters

Algebraic Analysis of the Poles in the Doppler Spectrum for Vehicle-to-Vehicle Channels

Michael Walter, *Senior Member, IEEE*, Dmitriy Shutin, *Senior Member, IEEE*, Armin Dammann, *Member, IEEE*

***Abstract*—In vehicle-to-vehicle wireless communications the time-variability of the propagation conditions is a challenge for channel estimation. The width of the Doppler spectrum depends on the propagation delay and the velocity vectors of the vehicles. So far, the time-variant width of the Doppler spectrum has been derived for single-bounce scattering close to the line-of-sight delay and for infinitely large delays. In this contribution, we generalize the time-variant, delay-dependent limiting frequencies for vehicle-to-vehicle channels for arbitrary delays and velocity vector configurations. The limiting frequencies are obtained by considering the geometric-stochastic channel representation in a prolate spheroidal coordinate system and determining the poles of the resulting Doppler spectrum. The poles in the spectrum are caused by the extrema of the Doppler frequency. Since the global maximum and minimum of the Doppler frequency define the limits of the spectrum, the time-variant, delay-dependent width can be calculated in closed form.**

***Index Terms*—V2V channel, geometry-based stochastic channel modeling, prolate spheroidal coordinates.**

I. Introduction

VEHICLE-TO-VEHICLE channels belong to the class of mobile-to-mobile (M2M) channels that are currently being actively studied amongst others in the framework of 5G communications technologies [1]. Understanding vehicle-to-vehicle (V2V) channels becomes particularly important in the perspective of novel transportation systems that depend on reliable data exchange for situation awareness. The standard wide sense stationary uncorrelated scattering (WSSUS) stochastic channel model was introduced by Bello in [2]. Shortly thereafter, the Doppler spectrum, which possesses two poles at the edges, for uniformly distributed scatterers for a moving receiver was derived in [3]. Subsequently, the Doppler spectrum for multi-bounce scattering was presented in [4] and it possesses also two poles for unequal vehicle speeds.

V2V channels, however, are characterized by their non-stationary behavior [5] and thus the validity of WSSUS models is limited to stationary scenarios. It has been shown in [6] that the class of geometric-stochastic channel models (GSCMs) are well suited to describe non-stationary channels. In [7], the authors propose a combination of line-of-sight (LOS) components, a two-sphere model, and multiple confocal elliptic-cylinder models to describe the non-stationary channel; a semi-ellipsoidal non-stationary channel model is proposed in [8]. Yet, analytical tractability of these GSCMs is limited. In contrast, the single-bounce ellipsoidal model in [9] permits a tractable analysis of non-stationary channels when expressed in a prolate spheroidal coordinate system (PSCS). In [10], the limiting frequencies for the Doppler spectrum close to the LOS and for infinite delay were derived in closed form. The results for arbitrary delays are, however, still elusive.

The authors are with the German Aerospace Center (DLR), Institute of Communications and Navigation, Wessling, 82234 Germany (e-mail: m.walter@dlr.de; dmitriy.shutin@dlr.de; armin.dammann@dlr.de).

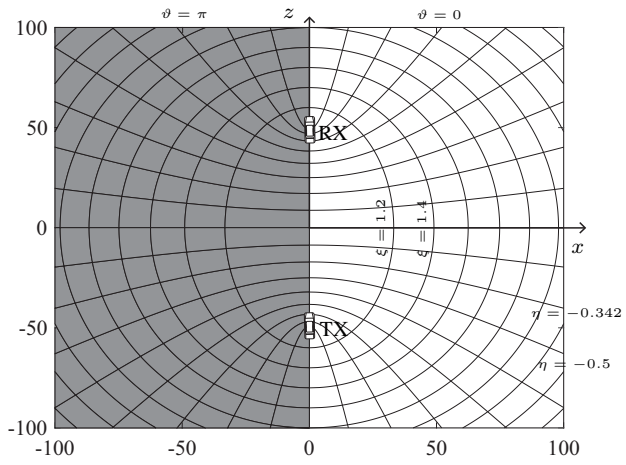

Fig. 1. Prolate spheroidal coordinate system with the transmitter and receiver in the foci of the ellipses and hyperbolas. The half-planes are given by $\vartheta = 0$ and $\vartheta = \pi$ (shaded). The relationship to the Cartesian coordinate system is displayed.

In this contribution we use PSCS to study the delay-dependent limiting frequencies. The use of PSCS allows us to conduct an algebraic analysis of the Doppler frequency. The performed analysis reveals a sixth order polynomial that describes poles of the time-variant, delay-dependent Doppler probability density function (pdf).

II. Prolate Spheroidal Coordinate System

An algebraic analysis of the Doppler spectrum in a Cartesian coordinate system is often prohibitively complex and cumbersome. Instead, the PSCS offers an elegant way to obtain algebraically tractable channel representations in terms of rational polynomials, which significantly simplify the analysis. As first discussed in [9], the PSCS is particularly suitable to solve two center problems, which are characteristic for the V2V channels as shown in Fig. 1.

The conversion between the Cartesian coordinate system and the PSCS is given according to [11] by

$$\begin{aligned} x &= l\sqrt{(\xi^2-1)(1-\eta^2)}\cos\vartheta\,, \\ y &= l\sqrt{(\xi^2-1)(1-\eta^2)}\sin\vartheta\,, \\ z &= l\xi\eta\,, \end{aligned} \tag{1}$$

This article has been accepted for publication in a future issue of this journal, but has not been fully edited. Content may change prior to final publication. Citation information: DOI 10.1109/LWC.2018.2810087, IEEE Wireless Communications Letters

where l is the focus distance, i.e., half the distance between transmitter (TX) and receiver (RX). The PSCS coordinates are defined as $\xi \in [1, \infty)$, $\eta \in [-1, 1]$, and $\vartheta \in [0, 2\pi)$. Note that iso-surfaces of the ξ-coordinate are ellipsoids. Here, $\xi \triangleq \frac{\tau}{\tau_{\mathrm{los}}}$ is the relative delay obtained by normalizing the propagation delay τ to the LOS delay τ_{los}. The distance d_{sc} from TX to RX via an arbitrary scatterer can be described by using only the ξ-coordinate as follows

$$d_{\mathrm{t}} = (\xi + \eta)\, l,\ d_{\mathrm{r}} = (\xi - \eta)\, l,\ d_{\mathrm{sc}} = d_{\mathrm{t}} + d_{\mathrm{r}} = 2\xi l\,, \quad (2)$$

where d_{t} is the distance from the TX to the scatterer, and d_{r} is the distance from the scatterer to the RX. The total delay is thus given by $\tau = \frac{d_{\mathrm{sc}}}{c} = \frac{2\xi l}{c}$, where c is the speed of light.

The Doppler frequency according to [9] is calculated as

$$f_{\mathrm{d}}(\mathbf{x}) = \left(\mathbf{v}_{\mathrm{t}}^{\mathrm{T}} \nabla d_{\mathrm{t}}(\mathbf{x}) + \mathbf{v}_{\mathrm{r}}^{\mathrm{T}} \nabla d_{\mathrm{r}}(\mathbf{x})\right) \frac{f_{\mathrm{c}}}{c}\,. \quad (3)$$

Here, the 3D instantaneous Doppler frequency is calculated by the gradient of the distance projected onto the velocity vectors of TX and RX. The expression in (3) can be recast in the PSCS according to [10] as

$$\begin{aligned} f_{\mathrm{d}}(t; \xi, \eta, \vartheta) = \Bigg(& \frac{\sqrt{(\xi^2 - 1)\,(1 - \eta^2)}}{\xi + \eta} \left(v_{\mathrm{t}x} \cos\vartheta + v_{\mathrm{t}y} \sin\vartheta\right) \\ & + \frac{\sqrt{(\xi^2 - 1)\,(1 - \eta^2)}}{\xi - \eta} \left(v_{\mathrm{r}x} \cos\vartheta + v_{\mathrm{r}y} \sin\vartheta\right) \\ & + \frac{\xi\eta + 1}{\xi + \eta} v_{\mathrm{t}z} + \frac{\xi\eta - 1}{\xi - \eta} v_{\mathrm{r}z} \Bigg) \frac{f_{\mathrm{c}}}{c}\,. \end{aligned} \quad (4)$$

Note that the Doppler frequency is a function of time due to time-dependency of the Cartesian components of the velocity vectors $\mathbf{v}_{\mathrm{t}} = [v_{\mathrm{t}x}, v_{\mathrm{t}y}, v_{\mathrm{t}z}]^{\mathrm{T}}$ and $\mathbf{v}_{\mathrm{r}} = [v_{\mathrm{r}x}, v_{\mathrm{r}y}, v_{\mathrm{r}z}]^{\mathrm{T}}$ of TX and RX, respectively. The 2D Doppler frequency for the V2V channel is then obtained by restricting the angle to $\vartheta \in \{0, \pi\}$.

We model the delay-dependent pdf of the uniformly distributed scatterers according to [9]. To this end, we fix the ξ-coordinate, which defines a certain delay ellipse. We further assume that for a fixed $\xi = \xi^*$ the scatterer distribution on the selected delay ellipse is independent of time t and consider the parameter $\eta \in [-1, 1]$ of the half-ellipse that specifies scatterers lying on it. It was shown in [9] that the conditional pdf $p(\eta|\xi)$ can be computed by applying standard rules of probability density transformations [12] as

$$p(\eta, \vartheta = 0|\xi) = p(\eta, \vartheta = \pi|\xi) = \frac{1}{2E\left(\frac{1}{\xi^2}\right)} \sqrt{\frac{1 - \frac{\eta^2}{\xi^2}}{1 - \eta^2}}\,, \quad (5)$$

where $E\left(\frac{1}{\xi^2}\right) \coloneqq \int_0^1 \sqrt{\frac{1 - \frac{\eta^2}{\xi^2}}{1 - \eta^2}}\, \mathrm{d}\eta$ is the complete elliptic integral of the second kind.

Following the derivation in [9], we compute the time-variant, delay-dependent Doppler pdf as

$$\begin{aligned} p(t; f_{\mathrm{d}}|\xi) = & \sum_{\eta' \in \{\mathcal{F}^{-1}(f_{\mathrm{d}})\}} \frac{1}{2} \frac{p(\eta, \vartheta = 0|\xi)}{\left|\frac{\partial f_{\mathrm{d}}(t;\eta,\vartheta=0|\xi)}{\partial\eta}\right|}\Bigg|_{\eta=\eta'} \\ & + \sum_{\eta' \in \{\mathcal{F}^{-1}(f_{\mathrm{d}})\}} \frac{1}{2} \frac{p(\eta, \vartheta = \pi|\xi)}{\left|\frac{\partial f_{\mathrm{d}}(t;\eta,\vartheta=\pi|\xi)}{\partial\eta}\right|}\Bigg|_{\eta=\eta'}\,, \end{aligned} \quad (6)$$

with the Doppler frequency $f_{\mathrm{d}}(t; \xi, \eta, \vartheta)$ being computed according to (4) and $\mathcal{F}^{-1}(\cdot)$ denoting the inverse relationship between η and f_{d}. The sum in (6) accounts for the fact that one Doppler frequency can be related to multiple values of η, which is sometimes referred to as a multivalued function. It can be shown, however, that there are at most four values of η that lead to the same Doppler frequency f_{d}.

III. Algebraic Analysis of the Doppler Spectrum

So far, a tractable analysis of the poles of $p(t; f_{\mathrm{d}}|\xi)$ has been done for delays close to the LOS and for infinitely large delays. In the following, we derive a general expression for the delay-dependent poles of the Doppler spectrum. Note that due to the physical limitation of the Doppler frequency in (4), the pdf $p(t; f_{\mathrm{d}}|\xi)$ has a finite support. From (6), it is obvious that the extrema of the Doppler frequency $f_{\mathrm{d}}(t; \eta, \vartheta, \xi)$ with respect to η lead to poles in the Doppler pdf; these naturally include minimum and maximum frequency of the Doppler pdf. Their location is given by

$$\frac{\partial f_{\mathrm{d}}(t; \xi, \eta, \vartheta)}{\partial \eta} = 0\,. \quad (7)$$

We expect that a least two poles will be located at the minimum and maximum Doppler frequency due to the physical limitation and continuity of the Doppler frequency. In the following, we investigate the algebraic structure of the poles and derive general properties of the Doppler spectrum. We begin with the following theorem.

Theorem 1. *In V2V channels the Doppler spectrum caused by single-bounce scattering can possess up to six distinct real poles.*

Proof. A straightforward computation of the derivative in (7) for both for $\vartheta = 0$ and $\vartheta = \pi$ leads to the following expression

$$\begin{aligned} \frac{\partial f_{\mathrm{d}}(t; \xi, \eta, \vartheta)}{\partial \eta} = \Bigg(& \mp \frac{\eta\left(\xi^2 - 1\right)}{(\xi + \eta)\sqrt{(\xi^2 - 1)\,(1 - \eta^2)}} v_{\mathrm{t}x} \\ & \mp \frac{\eta\left(\xi^2 - 1\right)}{(\xi - \eta)\sqrt{(\xi^2 - 1)\,(1 - \eta^2)}} v_{\mathrm{r}x} \\ & \mp \frac{\sqrt{(\xi^2 - 1)\,(1 - \eta^2)}}{(\xi + \eta)^2} v_{\mathrm{t}x} \\ & \pm \frac{\sqrt{(\xi^2 - 1)\,(1 - \eta^2)}}{(\xi - \eta)^2} v_{\mathrm{r}x} \\ & + \frac{\xi}{\xi + \eta} v_{\mathrm{t}z} - \frac{\xi\eta + 1}{(\xi + \eta)^2} v_{\mathrm{t}z} \\ & + \frac{\xi}{\xi - \eta} v_{\mathrm{r}z} + \frac{\xi\eta - 1}{(\xi - \eta)^2} v_{\mathrm{r}z} \Bigg) \frac{f_{\mathrm{c}}}{c} = 0\,. \end{aligned} \quad (8)$$

After isolating the expressions under the square root in (8), squaring the result, and taking the fact into account that solutions of (8) have to be combined for the cases $\vartheta = 0$ and $\vartheta = \pi$, the full set of solutions can be obtained as roots of the following polynomial in η as

$$g(\eta) = a_6\eta^6 + a_5\eta^5 + a_4\eta^4 + a_3\eta^3 + a_2\eta^2 + a_1\eta + a_0\,, \quad (9)$$

This article has been accepted for publication in a future issue of this journal, but has not been fully edited. Content may change prior to final publication. Citation information: DOI 10.1109/LWC.2018.2810087, IEEE Wireless Communications Letters

with coefficients a_i, $i = 0, \ldots, 6$, given as

$$\begin{aligned}
a_0 &= \left(\left(v_{\mathrm{t}x} - v_{\mathrm{r}x}\right)^2 + \left(v_{\mathrm{t}z} + v_{\mathrm{r}z}\right)^2 \right) \xi^4 - \left(v_{\mathrm{t}z} + v_{\mathrm{r}z}\right)^2 \xi^6 \\
a_1 &= 4 \left(v_{\mathrm{r}x}^2 - v_{\mathrm{t}x}^2 + v_{\mathrm{r}z}^2 - v_{\mathrm{t}z}^2\right) \xi^3 \\
&\quad + 2 \left(v_{\mathrm{t}x}^2 - v_{\mathrm{r}x}^2 + 2 \left(v_{\mathrm{t}z}^2 - v_{\mathrm{r}z}^2\right)\right) \xi^5 \\
a_2 &= \left(6 \left(v_{\mathrm{t}x}^2 + v_{\mathrm{r}x}^2 + v_{\mathrm{t}z}^2 + v_{\mathrm{r}z}^2\right) + 4 \left(v_{\mathrm{t}x} v_{\mathrm{r}x} - v_{\mathrm{t}z} v_{\mathrm{r}z}\right)\right) \xi^2 \\
&\quad + \left(2 v_{\mathrm{t}z} v_{\mathrm{r}z} - 8 \left(v_{\mathrm{t}x}^2 + v_{\mathrm{r}x}^2\right) - 7 \left(v_{\mathrm{t}z}^2 + v_{\mathrm{r}z}^2\right)\right) \xi^4 \\
&\quad + \left(\left(v_{\mathrm{t}x} + v_{\mathrm{r}x}\right)^2 + \left(v_{\mathrm{t}z} + v_{\mathrm{r}z}\right)^2 \right) \xi^6 \\
a_3 &= 4 \left(v_{\mathrm{r}x}^2 - v_{\mathrm{t}x}^2 + v_{\mathrm{r}z}^2 - v_{\mathrm{t}z}^2\right) \xi \\
&\quad + 4 \left(3 \left(v_{\mathrm{t}x}^2 - v_{\mathrm{r}x}^2\right) + 2 \left(v_{\mathrm{t}z}^2 - v_{\mathrm{r}z}^2\right)\right) \xi^3 \\
&\quad + 4 \left(v_{\mathrm{r}x}^2 - v_{\mathrm{t}x}^2 + v_{\mathrm{r}z}^2 - v_{\mathrm{t}z}^2\right) \xi^5 \\
a_4 &= \left(v_{\mathrm{t}x} - v_{\mathrm{r}x}\right)^2 + \left(v_{\mathrm{t}z} + v_{\mathrm{r}z}\right)^2 \\
&\quad + \left(2 v_{\mathrm{t}z} v_{\mathrm{r}z} - 8 \left(v_{\mathrm{t}x}^2 + v_{\mathrm{r}x}^2\right) - 7 \left(v_{\mathrm{t}z}^2 + v_{\mathrm{r}z}^2\right)\right) \xi^2 \\
&\quad + \left(6 \left(v_{\mathrm{t}x}^2 + v_{\mathrm{r}x}^2 + v_{\mathrm{t}z}^2 + v_{\mathrm{r}z}^2\right) - 4 \left(v_{\mathrm{t}x} v_{\mathrm{r}x} + v_{\mathrm{t}z} v_{\mathrm{r}z}\right)\right) \xi^4 \\
a_5 &= 2 \left(v_{\mathrm{t}x}^2 - v_{\mathrm{r}x}^2 + 2 \left(v_{\mathrm{t}z}^2 - v_{\mathrm{r}z}^2\right)\right) \xi \\
&\quad + 4 \left(v_{\mathrm{r}x}^2 - v_{\mathrm{t}x}^2 + v_{\mathrm{r}z}^2 - v_{\mathrm{t}z}^2\right) \xi^3 \qquad (10) \\
a_6 &= -\left(v_{\mathrm{t}z} + v_{\mathrm{r}z}\right)^2 + \left(\left(v_{\mathrm{t}x} + v_{\mathrm{r}x}\right)^2 + \left(v_{\mathrm{t}z} + v_{\mathrm{r}z}\right)^2 \right) \xi^2 .
\end{aligned}$$

According to the fundamental theorem of algebra, the polynomial $g(\eta)$ of degree 6 has exactly 6 roots; thus the number of poles in the V2V Doppler spectrum cannot exceed 6. □

If the sixth order polynomial is solvable, the general formula is provided in [13]. Let us stress that double roots can exist and that different roots of η can cause poles at the same Doppler frequency. Note that real roots can also be solutions of degenerate cases, e.g., for $v_{\mathrm{t}x} = v_{\mathrm{r}x} = 0$. The analysis, why the polynomial solves these cases as well, is, however, out of the scope of this paper.

Corollary 1. *If velocities of the TX and RX are such that $\|\mathbf{v}_\mathrm{t} + \mathbf{v}_\mathrm{r}\| \neq 0$, the V2V Doppler spectrum caused by a single-bounce scattering is characterized by either two, four or six real roots.*

Proof. Consider the coefficient a_6 in (10). It is easy to see that a_6 is zero if

$$\|\mathbf{v}_\mathrm{t} + \mathbf{v}_\mathrm{r}\| = 0, \quad \text{or} \quad \xi = \frac{v_{\mathrm{t}z} + v_{\mathrm{r}z}}{\|\mathbf{v}_\mathrm{t} + \mathbf{v}_\mathrm{r}\|} \leq 1. \qquad (11)$$

Since for single-bounce scattering $\xi > 1$, we can conclude that $a_6 \neq 0$ in this case. Thus, provided $\|\mathbf{v}_\mathrm{t} + \mathbf{v}_\mathrm{r}\| \neq 0$, $g(\eta)$ is a 6th order polynomial with real coefficients, with up to 6 real roots, or roots in complex conjugated pairs, from which the corollary follows. □

Corollary 2. *If $\|\mathbf{v}_\mathrm{t} + \mathbf{v}_\mathrm{r}\| = 0$, the V2V Doppler spectrum caused by single-bounce scattering can either have two or four real roots.*

Proof. In case when $\|\mathbf{v}_\mathrm{t} + \mathbf{v}_\mathrm{r}\| = 0$, the coefficients a_6, a_5, a_3 and a_1 become zero. Thus, the polynomial $g(\eta)$ reduces to a quartic polynomial with real coefficients a_4, a_2, and a_0. □

Note that, due to symmetry, the four real roots lead to only two poles at the maximum and minimum frequency in the Doppler spectrum. Let us analyze the generalization of the results in [10] for close to LOS and distant scattering.

A. Close to LOS Scattering ($\xi \to 1$)

Using Theorem 1, we can analyze the poles of the Doppler spectrum in the vicinity of the LOS. For $\xi \to 1$ and assuming six real roots, the following expressions for the six poles are obtained by solving (9) as

$$f_{1,2}(t) = \frac{v_{\mathrm{t}z} - v_{\mathrm{r}z}}{c} f_\mathrm{c}\,, \qquad (12)$$

$$f_{3,4}(t) = \frac{\pm\|\mathbf{v}_\mathrm{t}\| - v_{\mathrm{r}z}}{c} f_\mathrm{c}\,, \;\; f_{5,6}(t) = \frac{\pm\|\mathbf{v}_\mathrm{r}\| + v_{\mathrm{t}z}}{c} f_\mathrm{c}\,. \qquad (13)$$

These frequencies coincide exactly with the results obtained in [10]. Note that at $f_{1,2}(t)$ there is a double pole in the spectrum corresponding to the LOS frequency. It is found for $\eta \to \frac{v_{\mathrm{t}x} - v_{\mathrm{r}x}}{v_{\mathrm{t}x} + v_{\mathrm{r}x}}$ and the other four poles for $\eta \to \pm 1$.

B. Distant Scattering ($\xi \to \infty$)

Another limiting case is obtained for $\xi \to \infty$. As we have shown in [10], this relates to the situation when the Doppler pdf is reduced to the well-known Jakes spectrum shape in [3]. Again, using Theorem 1, it can be shown that for $\xi \to \infty$, the polynomial coefficients a_6, a_5, a_4, a_3, and a_1 behave as follows

$$\frac{a_6}{\xi^6} = o(\xi^{-3}),\; \frac{a_5}{\xi^6} = o(\xi^{-2}),\; \frac{a_4}{\xi^6} = o(\xi^{-1}),\; \frac{a_3}{\xi^6} = \frac{a_1}{\xi^6} = o(1). \qquad (14)$$

This implies that for large ξ, the coefficients a_2 and a_0 dominate the polynomial structure. As a result, (9) reduces to a quadratic polynomial for $\xi \to \infty$ with the two coefficients a_2 and a_0. A straight-forward analysis of (9) reveals that for $\eta \to \pm\frac{v_{\mathrm{t}z} + v_{\mathrm{r}z}}{\|\mathbf{v}_\mathrm{t} + \mathbf{v}_\mathrm{r}\|}$ the two limiting frequencies become

$$f_{7,8}(t) = \pm\frac{\|\mathbf{v}_\mathrm{t} + \mathbf{v}_\mathrm{r}\|}{c} f_\mathrm{c}\,. \qquad (15)$$

The result concurs with the two frequencies obtained in [10].

IV. Results

For our analysis, we purposely select a V2V scenario where six distinctive poles occur in the Doppler spectrum. The carrier frequency is $f_\mathrm{c} = 5.2\,\mathrm{GHz}$ and the Cartesian components of the velocity vectors of TX and RX are $\mathbf{v}_\mathrm{t} = [-90, 0, 0]^\mathrm{T}\mathrm{km/h}$ and $\mathbf{v}_\mathrm{r} = [-90, 0, 90]^\mathrm{T}\mathrm{km/h}$, respectively.

To get better insight in the structure of (4) and (8), we plot the Doppler frequency as a function of η for different, but fixed $\xi = \xi^*$ in Fig. 2. For $\xi = 1.0001$, i.e., close to the LOS and for $\eta \to \pm 1$, the f_d-curve reaches extreme values – these correspond to four of the total six poles in the Doppler pdf in (6). The frequencies of these extrema are given by (13). The other two extrema are obtained for $\eta \to \frac{v_{\mathrm{t}x} - v_{\mathrm{r}x}}{v_{\mathrm{t}x} + v_{\mathrm{r}x}} = 0$ and are effectively equivalent to a split of the LOS component, which is obtained for $\xi = 1$. Their frequencies are given by (12).

It can also be observed that the number of extrema decreases for increasing ξ. For $\xi = 1.0001$ and $\xi = 1.01$ six locations where the derivative in (7) becomes zero can be identified. For $\xi = 1.1$ only four locations can be found. As ξ continues to grow, e.g, for $\xi = 1000$, the number of poles drops to only two. The reason for such a behavior is the fact that for growing ξ, the 6th order polynomial begins to degenerate into a quadratic

This article has been accepted for publication in a future issue of this journal, but has not been fully edited. Content may change prior to final publication. Citation information: DOI 10.1109/LWC.2018.2810087, IEEE Wireless Communications Letters

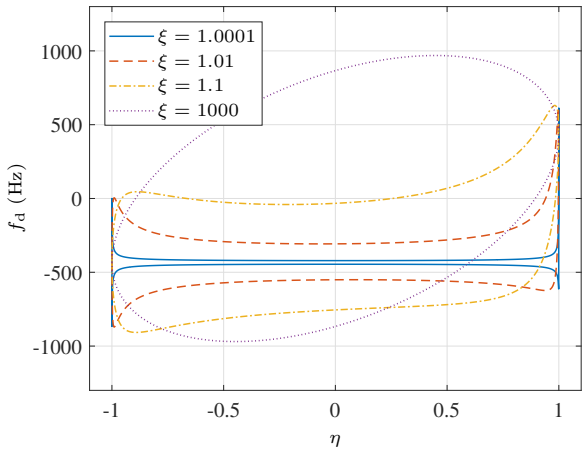

Fig. 2. Doppler frequency $f_\mathrm{d}\,(t^*;\xi^*,\eta,\vartheta^*)$ for vehicle velocity vectors $\mathbf{v}_\mathrm{t} = [-90,0,0]^\mathrm{T}\mathrm{km/h}$, $\mathbf{v}_\mathrm{r} = [-90,0,90]^\mathrm{T}\mathrm{km/h}$, and $\vartheta \in \{0,\pi\}$.

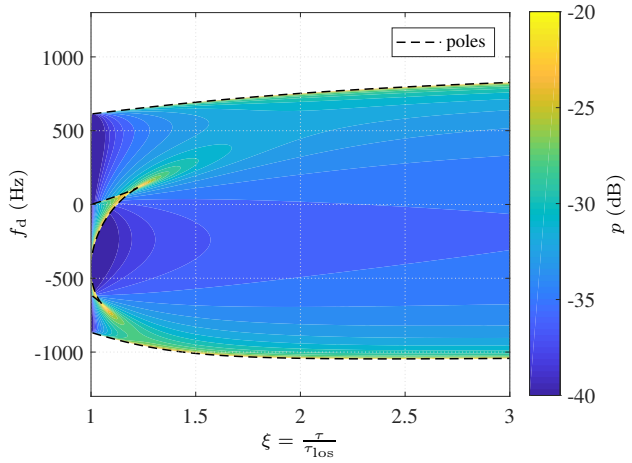

Fig. 3. Delay-dependent Doppler pdf $p(t^*;f_\mathrm{d}|\xi)$ and its delay-dependent poles (dashed line) for vehicle velocity vectors $\mathbf{v}_\mathrm{t} = [-90,0,0]^\mathrm{T}\mathrm{km/h}$ and $\mathbf{v}_\mathrm{r} = [-90,0,90]^\mathrm{T}\mathrm{km/h}$ with poles at $f_{1,2} = -433\,\mathrm{Hz}$, $f_3 = 0\,\mathrm{Hz}$, $f_4 = -867\,\mathrm{Hz}$, $f_5 = 613\,\mathrm{Hz}$, $f_6 = -613\,\mathrm{Hz}$ close to the LOS ($\xi \to 1$), and $f_{7,8} = \pm 969\,\mathrm{Hz}$ for large delays ($\xi \to \infty$).

polynomial with two extreme frequencies corresponding to the maximum and minimum Doppler frequency given by (15). Note that the number of distinct real roots of the polynomial in the half-open interval $(-1,1]$ can be found using Sturm's theorem [14]. According to Sturm's theorem the number of distinct real roots of the polynomial decreases from six to four, and then from four to two. The number of real roots in this particular scenario corresponds exactly to the number of poles in the Doppler spectrum.

The delay-dependent Doppler pdf $p(t;f_\mathrm{d}|\xi)$ is shown in Fig. 3 for a fixed time instance $t = t^*$. The locations of the delay-dependent poles of the Doppler spectrum for an arbitrary delay ξ are displayed as dashed lines in Fig. 3. Close to the LOS, i.e., for $\xi = 1.0001$, there are six poles in the Doppler spectrum computed by (12) and (13). As we increase ξ away from the LOS delay, the positions of the poles are determined numerically using the polynomial in (9). At $\xi \approx 1.051$ the number of poles drops from six to four and at $\xi \approx 1.224$ from four to two, also confer Fig. 2. For large delays, we observe a Jakes-like symmetric Doppler spectrum with only two poles remaining, which denote the minimum and maximum Doppler frequency. These frequencies are calculated by (15). Thus, our findings concur the known results in the literature and generalize them.

V. Conclusion

We have investigated the algebraic structure of the poles in the Doppler spectrum for arbitrary delays and velocity configurations for single-bounce scattering in a prolate spheroidal coordinate system. The performed analysis permitted deriving a theorem with the maximum number of poles in the vehicle-to-vehicle Doppler spectrum. Specifically, we proved that the Doppler spectrum has at most six poles. Their locations are determined by a 6th order polynomial. Two of the poles naturally reflect the minimum and maximum frequency of the Doppler spectrum. The other poles occur inside the delay-dependent Doppler probability density function relatively close to the LOS delay. For large delays only two of the six poles remain in the spectrum.

References

[1] M. N. Tehrani, M. Uysal, and H. Yanikomeroglu, "Device-to-device communication in 5G cellular networks: challenges, solutions, and future directions," *IEEE Commun. Mag.*, vol. 52, no. 5, pp. 86–92, May 2014.

[2] P. Bello, "Time-frequency duality," *IEEE Trans. Inform. Theory*, vol. 10, no. 1, pp. 18–33, Jan. 1964.

[3] R. H. Clarke, "A statistical theory of mobile-radio reception," *Bell Syst. Tech. J.*, vol. 47, no. 6, pp. 957–1000, Jul./Aug. 1968.

[4] A. S. Akki and F. Haber, "A statistical model of mobile-to-mobile land communication channel," *IEEE Trans. Veh. Technol.*, vol. 35, no. 1, pp. 2–7, Feb. 1986.

[5] L. Bernadó, T. Zemen, F. Tufvesson, A. F. Molisch, and C. F. Mecklenbräuker, "The (in-) validity of the WSSUS assumption in vehicular radio channels," in *Proc. IEEE 23rd Int. Symp. Personal, Indoor and Mobile Radio Commun. (PIMRC)*, Sydney, NSW, Australia, Sep. 2012, pp. 1757–1762.

[6] A. F. Molisch, F. Tufvesson, J. Karedal, and C. F. Mecklenbräuker, "A survey on vehicle-to-vehicle propagation channels," *IEEE Wireless Commun. Mag.*, vol. 16, no. 6, pp. 12–22, Dec. 2009.

[7] Y. Yuan, C.-X. Wang, Y. He, M. M. Alwakeel, and e. H. M. Aggoune, "3D wideband non-stationary geometry-based stochastic models for non-isotropic MIMO vehicle-to-vehicle channels," *IEEE Trans. Wireless Commun.*, vol. 14, no. 12, pp. 6883–6895, Dec. 2015.

[8] H. Jiang, Z. Zhang, J. Dang, and L. Wu, "A novel 3-D massive MIMO channel model for vehicle-to-vehicle communication environments," *IEEE Trans. Commun.*, vol. 66, no. 1, pp. 79–90, Jan. 2018.

[9] M. Walter, D. Shutin, and U.-C. Fiebig, "Prolate spheroidal coordinates for modeling mobile-to-mobile channels," *IEEE Antennas Wireless Propagat. Lett.*, vol. 14, pp. 155–158, 2015.

[10] M. Walter, D. Shutin, and A. Dammann, "Time-variant Doppler PDFs and characteristic functions for the vehicle-to-vehicle channel," *IEEE Trans. Veh. Technol.*, vol. 66, no. 12, pp. 10 748–10 763, Dec. 2017.

[11] C. Flammer, *Spheroidal Wave Functions*. Stanford, CA: Stanford University Press, 1957.

[12] W. Davenport and W. Root, *An introduction to the theory of random signals and noise*, ser. Lincoln Laboratory publications. McGraw-Hill, 1958.

[13] T. R. Hagedorn, "General formulas for solving solvable sextic equations," *Journal of Algebra*, vol. 233, no. 2, pp. 704 – 757, 2000.

[14] C. F. Sturm, "Analyse d'un mémoire sur la résolution des équations numériques," *Bulletin de Férussac*, vol. XI, no. 271, pp. 419–422, 1829.